ELSEVIER

Journal of Alloys and Compounds 446–447 (2007) 242–247

Journal of ALLOYS AND COMPOUNDS

www.elsevier.com/locate/jallcom

Raman scattering and lattice stability of $NaAlH_4$ and Na_3AlH_6

H. Yukawa [a,*], N. Morisaku [a], Y. Li [a], K. Komiya [a], R. Rong [a], Y. Shinzato [a], R. Sekine [b], M. Morinaga [a]

[a] *Department of Materials Science and Engineering, Graduate School of Engineering, Nagoya University, Chikusa-Ku, Nagoya 464-8603, Japan*

[b] *Department of Chemistry, Faculty of Science, Shizuoka University, 836 Ohya, Shizuoka 422-8529, Japan*

Received 29 September 2006; received in revised form 13 February 2007; accepted 14 February 2007
Available online 20 February 2007

Abstract

In situ Raman spectroscopy measurements have been performed during the decomposition of $NaAlH_4$ in order to investigate the transition from the four-coordinated complex anion, $[AlH_4]^-$, in $NaAlH_4$ to the six-coordinated complex anion, $[AlH_6]^{3-}$, in Na_3AlH_6. Also, the local geometry and the Al–H vibrations are analyzed theoretically by the first-principle calculations of the electronic structures. It is found that the Raman sift at 1765 cm^{-1} for the Al–H stretching vibration in $NaAlH_4$ shifts towards the higher frequency side, 1801 cm^{-1} upon melting. This Raman spectrum for the liquid phase recovers to the original position when it is cooled down to room temperature before Na_3AlH_6 start to appear. The Raman peak around 1800 cm^{-1} is still observed after the decomposition of $NaAlH_4$ occurs to precipitate Na_3AlH_6. However, this peak does not recover to its original position by cooling, but still persists in the sample cooled down to room temperature. From these results, the intermediate transition state during the decomposition of $NaAlH_4$ into Na_3AlH_6 is discussed. In addition, it is shown from a series of calculation that the highest frequency of the Al–H vibration correlates with the shortest Al–H bond length in the $MAlH_4$-type and its derivative complex hydrides.

Keywords: Hydrogen storage materials; Complex hydride; Raman spectroscopy; Al–H vibration; First-principle calculation

1. Introduction

Recently, special attention has been directed toward complex hydrides, such as $NaAlH_4$, $LiNH_2$ and $LiBH_4$, because they are superior in both the gravimetric and volumetric densities of hydrogen to conventional hydrogen storage alloys. However, for these complex hydrides, there are still some problems in the reversibility of hydrogenation and dehydrogenation reactions, and also in high decomposition temperatures and low reaction rates. Bogdanović and Schwickardi first demonstrated that the doping of Ti catalyst enhances the kinetic and reversibility of hydrogen absorption and desorption reaction of $NaAlH_4$ [1]. Then, an extensive study has been made on the alanate systems experimentally and theoretically [2–6].

Uncatalyzed $NaAlH_4$ melts at 453 K [7], and then releases hydrogen to form Na_3AlH_6 by the following reaction,

$$NaAlH_4 \leftrightarrow \tfrac{1}{3}(Na_3AlH_6) + \tfrac{2}{3}Al + H_2. \quad (1)$$

Through this reaction, the four-coordinated complex anion, $[AlH_4]^-$, in $NaAlH_4$ transforms into the six-coordinated complex anion, $[AlH_6]^{3-}$, in Na_3AlH_6. The process of this transition will be important to the understanding of the alanate-type complex hydride for hydrogen storage.

Raman spectroscopy measurements have been carried out in order to investigate the Al–H vibrations in $NaAlH_4$ and Na_3AlH_6 [8,9]. The Al–H symmetric and anti-symmetric stretching vibrations appear at 1761 and 1682 cm^{-1} for $NaAlH_4$ [8], and at 1556 and 1152 cm^{-1} for Na_3AlH_6 [9], respectively. *In situ* Raman spectroscopy measurements have also been performed [2]. A significant softening was observed in the tranlations and librations modes of $[AlH_4]^-$ anion during the heating up to 425 K. On the other hand, the frequencies of the Al–H stretching and bending vibration modes were nearly constant indicating that

* Corresponding author.
E-mail address: hiroshi@numse.nagoya-u.ac.jp (H. Yukawa).

0925-8388/$ – see front matter © 2007 Elsevier B.V. All rights reserved.
doi:10.1016/j.jallcom.2007.02.071

the $[AlH_4]^-$ anion is a stable unit up to the melting temperature. In fact, the Al–H stretching mode was persisted in the surface melted sample at the temperature slightly below the melting point even after the signal from the $NaAlH_4$ lattice was lost [2].

The phase transition during reaction (1) has also been studied by *in situ* X-ray diffraction measurements [10,11]. Gross et al. reported that an unknown phase, X_1, with a cubic symmetry starts to precipitate just after $NaAlH_4$ melts at 453 K [10]. However, no such intermediate phase was observed in the experiments performed by Balogh et al. [11]. On the other hand, the Raman spectrum during the decomposition of $NaAlH_4$ has not been investigated.

There is a recent idea that the transformation of $NaAlH_4$ into Na_3AlH_6 proceed through the formation of NaH-like and AlH_3-like local structure [10]. More recently, Fu et al. suggest from their high-resolution inelastic neutron scattering measurements that a volatile molecular aluminum hydride, such as AlH_3 may be formed during the early stage of H_2 regeneration of a deplated, catalyzed $NaAlH_4$ [12]. However, the details of the transition state during the decomposition of $NaAlH_4$ still remain unclear.

In this study, the transition from $NaAlH_4$ to Na_3AlH_6 is investigated experimentally by using *in situ* Raman spectroscopy. Also, for comparison, the Raman spectra for $LiAlH_4$ and $KAlH_4$ are measured at room temperature. In addition, the Raman spectrum and the Al–H vibrations as well as the local geometries of the hydrides are investigated theoretically by the first-principal calculation of the electronic structures.

2. Experimental procedure

2.1. In situ Raman spectroscopy for purified $NaAlH_4$

Powder of $NaAlH_4$ (90%) is purchased from Sigma–Aldrich Inc. The purified sample is prepared by the method mentioned in literature [1,13]. Namely, about 10 g of $NaAlH_4$ is dissolved into about 100 ml of dehydrated THF (less than 50 ppm H_2O) and then it is stirred for 10.8 ks (3 h). The supernatant liquid of the mixture is decanted using a syringe and concentrated in vacuo to the volume of ~20 ml. Then, 80 ml of dehydrated pentane (less than 10 ppm H_2O) is added to the THF solution causing $NaAlH_4$ to separate from the solution as a fine precipitate. The suspension is stirred for 3.6 ks (1 h) and the supernatant is removed. The precipitate is washed two times with pentane and dried in vacuo to obtain a fine colorless power of $NaAlH_4$.

In a glove box filled with a purified argon gas (dew point below 183 K), the sample is set on a gastight stage equipped with a heating unit. The temperature is controlled by a thermocouple set on the heating stage. After the sample reached to the measuring temperature, keep for 900 s or 1.8 ks, then the *in situ* Raman spectroscopy measurements are performed at each isothermal condition with a 532 nm excitation laser using a 600 grooves/mm grating, focused at 2200 cm^{-1}. The spectrum is measured in the range between 137 and 3822 cm^{-1}, within the accuracy of about $\pm 12\ cm^{-1}$.

2.2. Raman spectroscopy for $MAlH_4$ (M = Li, Na, K)

$KAlH_4$ is prepared by mechanical ball milling. Powders of $LiAlH_4$ (95%), KH (dispersed in a mineral oil) and Al (99.95%) are purchased form Sigma–Aldrich Inc. In a glove box, KH is washed several times with purified hexane to separate KH from the oil, followed by the evaporation of the solvent. Powders of KH and Al are mixed by a mole ratio of 1:1 to obtain an initial mixture. About 300 mg of the mixture is put into a Cr-steel pot together with 20 pieces of steel balls with a diameter of 6.5 mm. Then, the pot is evacuated and about 1.0 MPa of hydrogen is introduced. The sample is mechanically milled by a planetary ball-milling apparatus (Fritsch P7) with 400 rpm for 72 ks (20 h) at an ambient temperature. Subsequently, it is heat treated at 573 K for 72 ks (20 h) under a hydrogen pressure of 1.2 MPa. The Raman spectroscopy measurements for $MAlH_4$ (M = Li, Na, K) are carried out at room temperature.

3. Calculation

3.1. Theoretical Raman spectrum for $NaAlH_4$

The theoretical Raman spectrum for $NaAlH_4$ is simulated by using the Gaussian 03 [14]. The DFT calculation is performed using B3LYP method as implemented in the package. The 6–31+g(d,p) bases set is used in the calculation. The cluster model used is $[Na_8(AlH_4)_9]^-$ which is constructed on the basis of the crystal structure of $NaAlH_4$ [15]. In this model, an $[AlH_4]^-$ anion is located at the center and it is surrounded by eight Na^+ cations and eight $[AlH_4]^-$ anions. The total charge of the cluster is set to be −1. Fixing the positions of the surrounding ions, the local geometry of the central AlH_4 is optimized. The theoretical Raman spectrum is examined for the Al–H vibration of the central AlH_4.

3.2. Analysis of the Al–H vibration

The other calculations are also performed for $NaAlH_4$, $LiAlH_4$, $KAlH_4$, Na_3AlH_6 and Li_3AlH_6 in order to analyze the Al–H vibration at the highest frequency of the normal mode. The plane wave pseudo potential method (program code CASTEP [16]) is used in this study. The super cell is constructed on the basis of the crystal structure of each hydride [17–20] and employed in the calculation with the periodic boundary condition of the crystal lattice. The norm-conserving pseudo potentials are used and the cut-off energy is set to be 770 eV so that the total energy converges within 0.0001 eV per atom for each calculation. The lattice parameters as well as the local geometries are fully optimized by minimizing the total energy, and the Al–H vibration mode at the Γ point is analyzed from the calculation.

4. Results and discussion

4.1. In situ Raman spectroscopy measurement

In situ Raman spectroscopy measurements are conducted by heating $NaAlH_4$ under an argon gas atmosphere. The results of the Raman spectra are shown in Fig. 1. The Raman spectrum obtained at room temperature shown in Fig. 1(a) is in good agreement with the previous results [2,8]. The spectrum is divided mainly into three frequency regions around 500, 800 and 1700 cm^{-1}. As shown in Fig. 1(a–c-1), the peaks around 500 cm^{-1} shift towards lower frequency side and became weaker with increasing the temperature. On the other hand, the peaks around 800 and 1700 cm^{-1} are scarcely changed during the heating up to 458 K. These results are in good agreement with the previous work [2].

When the sample is heated and kept at 458 K for 1.8 ks, the peaks around 500 cm^{-1} disappears as shown in Fig. 1(c-2). Simultaneously, the main peak at 1765 cm^{-1} shifts toward

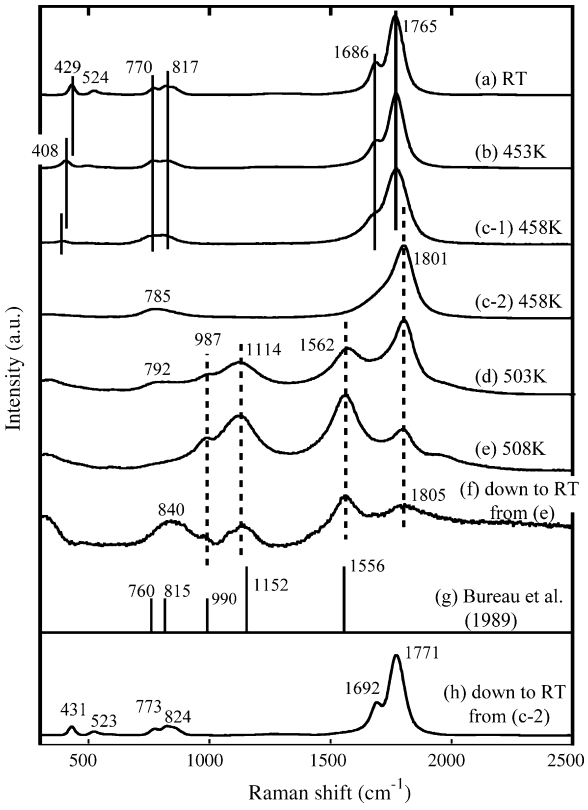

Fig. 1. *In situ* Raman spectra of $NaAlH_4$ measured at each isothermal condition under argon gas atmosphere. Typical measurements except for (c-2) are performed 900 s after the temperature reached to each condition. (a) R.T., (b) 453 K, (c-1) 458 K, (c-2) 458 K after 1.8 ks, (d) 503 K, (e) 508 K, (f) down to R.T. from 508 K, (h) down to R.T. from 458 K (c-2). Reported Raman frequencies and relative intensities for Na_3AlH_6 is drawn in (g) [9].

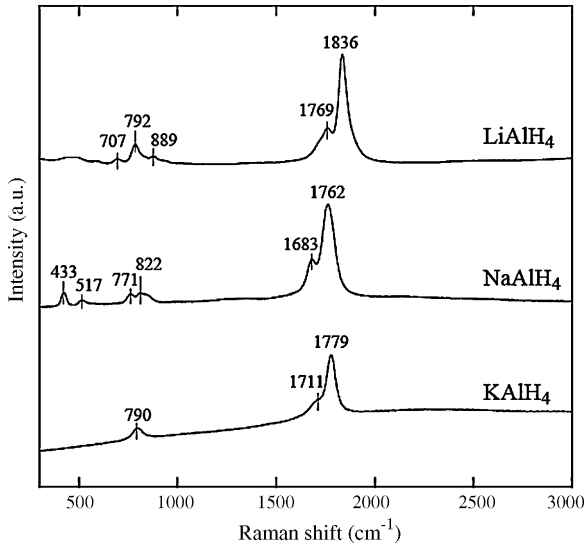

Fig. 2. Raman spectra for $MAlH_4$ (M = Li, Na, K) measured at room temperature under argon gas atmosphere.

higher frequency side. At the same time, the peak at 1686 cm^{-1} becomes unclear. All the peaks recover to their original position after the sample is cooled down to room temperature from this condition, as shown in Fig. 1(h). It is stressed that the Raman spectrum shown in Fig. 1(c-2) is somewhat different from the one reported by Majzob et al. for the surface melted single crystal of $NaAlH_4$, where the Raman frequency of the main peak for Al–H stretching vibration scarcely changed even after the $NaAlH_4$ lattice was lost [2].

On the other hand, when the sample is heated to 503 K, new peaks appear at 1562, 1114 and 987 cm^{-1} as shown in Fig. 1(d). These peaks are in good agreement with the reported Raman frequencies for Na_3AlH_6 as shown in Fig. 1(g) [9]. According to the previous study, these new peaks correspond to the stretching and bending vibration of H in Na_3AlH_6, respectively [9]. Above 503 K, there is no significant change in the Raman spectrum, although the relative intensity of the peak around 1800 cm^{-1} decreases with increasing temperature as shown in Fig. 1(e). The peaks around 800 cm^{-1} are still visible at 503 K but they diminish at 508 K.

Fig. 1(f) shows the Raman spectrum for the sample cooled down from 508 K to room temperature. A relatively large peak appears at 840 cm^{-1}. However, the frequencies for all the other peaks are nearly the same as those obtained from the sample at 508 K shown in Fig. 1(e). It is important to note that the peak around 1800 cm^{-1} still remains.

4.2. Raman spectrum for $MAlH_4$ (M = Li, Na, K)

The Raman spectra for $MAlH_4$ (M = Li, Na, K) at room temperature are shown in Fig. 2. The Raman spectrum for $LiAlH_4$ is in good agreement with the previous work [21]. The Al–H stretching and the Al–H–M bending vibrations are clearly observed for each spectrum. The main peak appears at the highest frequency changes in the order, $LiAlH_4$ (1836 cm^{-1}) > $KAlH_4$ (1779 cm^{-1}) > $NaAlH_4$ (1762 cm^{-1}), which is different from the order of elements (Li, Na, K) in the periodic table. A similar trend is also seen for the second peak existing around 1700 cm^{-1}.

4.3. Theoretical Raman spectrum for $NaAlH_4$

Fig. 3 shows the calculated Raman spectrum for $NaAlH_4$ obtained by using the Gaussian 03. The cluster model shown in the inset of the figure is employed in the calculation. Here, the scaling factor of 0.9613 [22] is used to correct the calculated frequencies of the Al–H vibration. As shown in Fig. 3, the experimental Raman spectrum for $NaAlH_4$ at room temperature shown in Fig. 1(a) is well reproduced by the simulation. For example, the measured peaks at 1762 cm^{-1} and 1683 cm^{-1} correspond to the Al–H symmetric and anti-symmetric stretching modes, respectively. Also, the peaks appeared around 800 cm^{-1} attribute to the Al–H–Na bending vibration modes. In addition, the peaks around 500 cm^{-1} correspond to the libration of $[AlH_4]^-$ anion.

However, further cluster calculation with the Gaussian 03 is difficult for Na_3AlH_6. This is because the crystal symmetry around Al in Na_3AlH_6 is lower than that in $NaAlH_4$. Therefore, the optimization of the positions of H atoms around Al, which is an important process in calculating the theoretical Raman

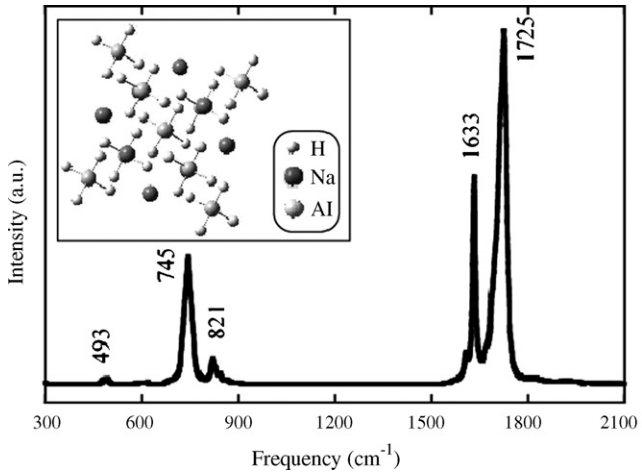

Fig. 3. Calculate Raman spectrum for $NaAlH_4$. The inset is the cluster model used in the calculation.

spectrum, results in the unreal arrangements in use of a finite size of cluster model.

4.4. Al–H stretching vibration at the highest frequency

Then, further analysis of the Al–H vibration mode is performed using the plane wave pseudo potential method with the periodic boundary condition of the crystal lattice. For comparison, the calculations are also conducted for the other series of alanate hydrides, $LiAlH_4$, $KAlH_4$ and Li_3AlH_6. Here, the scaling factor of 0.97 is used to estimate the frequency number from the calculation.

In this study, we focus on the Al–H stretching vibration at the highest frequency of the normal mode, and the results are shown in the parentheses in Fig. 4. The calculated frequency for each hydride is in good agreement with experiments. For example, the frequency changes in the order, $LiAlH_4$ (1861 cm^{-1}) > $KAlH_4$ (1800 cm^{-1}) > $NaAlH_4$ (1753 cm^{-1}), in consistent with the experimental results shown in Fig. 2. It is noted that the frequencies for the AlH_6-type hydrides (1590 cm^{-1} for Li_3AlH_6 and 1505 cm^{-1} for Na_3AlH_6) are much lower than those for the AlH_4-type hydrides.

Fig. 4 shows the schematic illustration of the $[AlH_4]^-$ and $[AlH_6]^{3-}$ complex anion in each hydride. The Al–H vibration modes at the highest frequency and the corresponding Al–H interionic distances for each hydride are shown in the figure. For $NaAlH_4$, as shown in Fig. 4(b), all the Al–H bonds have the same interionic distance of 0.1622 nm. This is due to the fact that the symmetry of the crystal structure of $NaAlH_4$ is high around Al so the four H atoms around Al are equivalent in it. Therefore, all the four H atoms around Al vibrate in a symmetric and harmonic stretching mode at the highest frequency of 1753 cm^{-1} as shown in Fig. 4(b).

On the other hand, for $LiAlH_4$ and $KAlH_4$, the Al–H distances in the hydrides vary to some extent. This is because the crystal lattice is distorted around Al due to the low symmetry of the crystal structure for these hydrides. In this case, the hydrogen atom with shorter Al–H bond tends to vibrate primarily at

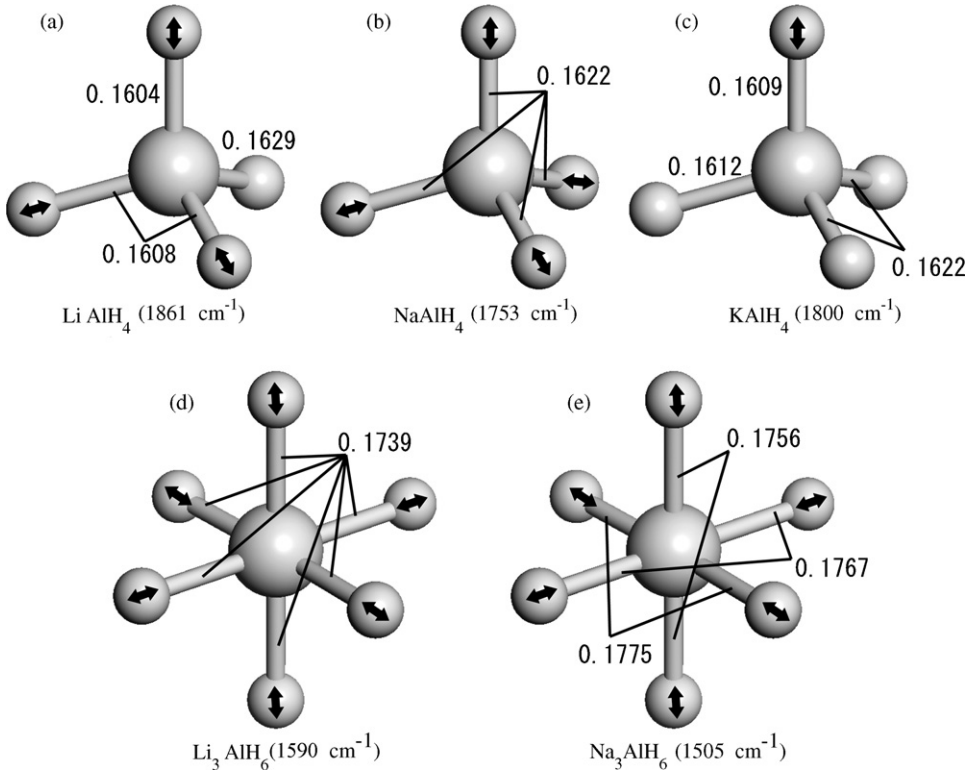

Fig. 4. Schematic illustration of the Al–H vibration mode in the complex anions in: (a) $LiAlH_4$ (1861 cm^{-1}), (b) $NaAlH_4$ (1753 cm^{-1}), (c) $KAlH_4$ (1800 cm^{-1}), (d) Li_3AlH_6 (1590 cm^{-1}) and (e) Na_3AlH_6 (1505 cm^{-1}). The Al–H bond distances (nm) and the highest frequency of the normal mode are also shown in the figure.

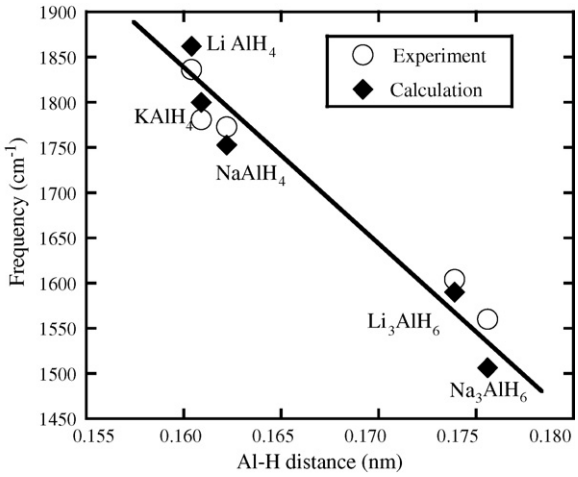

Fig. 5. Correlation between the highest frequency of the normal mode and the shortest bond distance in the hydrides.

the highest frequency. For example, in case of $LiAlH_4$, three H atoms with the shorter Al–H distances of 0.1604 and 1.608 nm mainly vibrate with the highest frequency, 1861 cm^{-1}, in a harmonic stretching mode as shown in Fig. 4(a). Similarly, in case of $KAlH_4$, only one H atom with the shortest Al–H distance of 0.1609 vibrates at 1800 cm^{-1}.

For Li_3AlH_6 and Na_3AlH_6, the Al–H interionic distances are significantly longer than those for the AlH_4-type alanate hydrides. All the six H atoms around Al vibrate in a symmetric and harmonic stretching mode at the highest frequency, as shown in Fig. 4(d and e).

Fig. 5 shows the correlation between the shortest Al–H interionic distance and the highest frequency of the normal mode of the Al–H stretching vibration for each hydride. There is a tendency that the highest frequency number increases with decreasing the shortest Al–H interionic distance in the hydride. Similar results are also reported for BD_4-type complex deuterides, where the frequency of the B–D stretching vibration correlates with the B–D bond length in alkali borodeuterides MBD_4 (M = Na, K, Rb, Cs) [23].

4.5. Raman spectrum of liquid $NaAlH_4$ and intermediate transition state

As shown in Fig. 1(c-2), when the sample is heated and kept at 458 K, just above the melting point, the highest Raman peak for the Al–H stretching vibration shifts toward the higher frequency side. Simultaneously, the signal from the lattice disappears. This change in the Raman spectrum can be attributable to the melting of $NaAlH_4$. In fact, as shown in Fig. 1(h), the Raman spectrum is completely recovers when the sample is cooled down to room temperature from this condition before Na_3AlH_6 appears.

On the other hand, the Raman peak at 1800 cm^{-1} observed at 508 K shown in Fig. 1(e) may not correspond to the liquid state of $NaAlH_4$. This is because, as shown in Fig. 1(f), the peak at 1800 cm^{-1} still persists in the sample cooled down to room temperature from 508 K. It is likely that a new intermediate state which is stable even at room temperature seems to appear during the decomposition of $NaAlH_4$. As mentioned before, $NaAlH_4$ decomposes to form Na_3AlH_4 through reaction (1). Through this reaction, the tetrahedral complex anion, $[AlH_4]^-$, in $NaAlH_4$ transforms into the octahedral complex anion, $[AlH_6]^{3-}$, in Na_3AlH_6. As the coordination numbers and geometries are quite different from each other between these polyhedra, it is reasonable to consider the intermediate state during the transition from $NaAlH_4$ to Na_3AlH_6.

As explained before, $[AlH_4]^-$ anion is considered to be a stable unit even after the $NaAlH_4$ lattice is lost [2]. Therefore, one may speculate that Na^+ cation interacts with $[AlH_4]^-$ anion in the liquid $NaAlH_4$ without any constrain from the crystal lattice. This will modify the local structure of $[AlH_4]^-$ anion. The positions of the peak at 1800 cm^{-1} are very similar between Fig. 1(c-2 and e), suggesting a similar local structure of $[AlH_4]^-$ exist both in the liquid $NaAlH_4$ and in the sample cooled down to room temperature from 508 K. In other words, the intermediate state appeared during the decomposition is seemed to be composed of essentially the similar local structure of the modified $[AlH_4]^-$ anion exist in the liquid phase.

Recently, Gross et al. proposed that the transformation of $NaAlH_4$ into Na_3AlH_6 proceed through the formation of NaH-like and AlH_3-like local structure [10]. In fact, $NaAlH_4$ can be synthesized indirectly by mixing Na_3AlH_6 or NaH with AlH_3 in THF solution [24,25]. Fu et al. reported from their high-resolution inelastic neutron scattering measurements that a volatile molecular aluminum hydride forms during the early stage of H_2 regeneration of $NaAlH_4$ [12]. They suggested the formation of AlH_3 (and oligomers $(AlH_3)_n$) play an important role in the hydrogen absorption and desorption reactions of $NaAlH_4$.

Assuming that Na^+ interacts one of four H^- in $[AlH_4]^-$ and a local structure of ($NaH–AlH_3$) appears in the liquid $NaAlH_4$, the distorted AlH_3 species may be one possibility to explain the change in the Raman spectrum upon melting. It is noted here that the AlH_3 species might be favorable in view of the geometrical transition from the four-coordinated $[AlH_4]^-$ anion to the six-coordinated $[AlH_6]^{3-}$ anion. This is because AlH_3 polymers tend to form a structure containing octahedral AlH_6 unit in it. In fact, α-AlH_3 is known to have a trigonal crystal structure (space group $R\bar{3}c$) and is composed of the corner-sharing AlH_6 octahedra [26,27]. Similarly, γ-AlH_3 is reported to contain the edge-sharing AlH_6 octahedral unit [28].

However, the origin of the Raman spectrum at 1800 cm^{-1} still remains unclear. Additional experiments will be needed to the understanding of the transition state during the decomposition of $NaAlH_4$.

5. Summery

The transition from the four-coordinated complex anion, $[AlH_4]^-$, in $NaAlH_4$ to the six-coordinated complex anion, $[AlH_6]^{3-}$, in Na_3AlH_6 is investigated experimentally by using *in situ* Raman spectroscopy. Also, the Al–H vibration is analyzed theoretically by using the Gaussian 03 and the CASTEP programs.

It is found that the Raman peak for the Al–H stretching vibration of $NaAlH_4$ shifts toward the higher frequency side upon

melting. This Raman spectrum recovers to the original position by cooling the sample to room temperature before $NaAlH_4$ start to decompose. However, once the decomposition of $NaAlH_4$ takes place and Na_3AlH_6 start to appear, the Raman peak at $1800\,cm^{-1}$ does not recover by cooling but it persists even in the sample cooled down to room temperature. From these results, the intermediate transition state during the decomposition of $NaAlH_4$ into Na_3AlH_6 is discussed. Also, from a series of calculations, it is shown that the highest frequency at the normal mode of the Al–H stretching vibration correlates with the shortest Al–H bond length in the $MAlH_4$-type and its derivative complex hydrides.

Acknowledgements

The authors would like to express sincere thanks to the staffs of the Computer Center, Institute for Molecular Science, Okazaki National Institute for the use of supercomputers. This study was supported by a Grant-in-Aid for Scientific Research from the Ministry of Education, Culture, Sports, Science and Technology of Japan, by the Japan Society for the Promotion of Science, and also by the 21st Century COE Program "Nature-Guided Materials Processing" of the Ministry of Education, Culture, Sports, Science and Technology.

References

[1] B. Bogdanović, M. Schwickardi, J. Alloys Compd. 253–254 (1997) 1.
[2] E.H. Majzoub, K.F. McCarty, V. Ozliņš, Phys. Rev. B 71 (2005) 024118.
[3] M. Fichtner, O. Fuhr, O. Kircher, J. Alloys Compd. 356–357 (2003) 418.
[4] F. Fossdal, H.W. Brinks, J.E. Fonneløp, B.C. Hauback, J. Alloys Compd. 397 (2005) 135.
[5] M.E. Arroyo y de Dompablo, G. Ceder, J. Alloys Compd. 364 (2004) 6.
[6] M. Yoshino, K. Komiya, Y. Takahashi, Y. Shinzato, H. Yukawa, M. Morinag, J. Alloys Compd. 404–406 (2005) 185.
[7] P. Claudy, B. Bonnetot, G. Chahine, J.M. Letoffe, Thermochim. Acta 38 (1980) 75.
[8] S. Gomes, G. Renaudin, H. Hagemann, K. Yvon, M.P. Sulic, C.M. Jensen, J. Alloys Compd. 390 (2005) 305.
[9] J.C. Bureau, Z. Amri, P. Claudy, J.M. Létoffé, Mater. Res. Bull. 24 (1989) 23.
[10] K.J. Gross, S. Guthrie, S. Takara, G. Thomas, J. Alloys Compd. 297 (2000) 270.
[11] M.P. Balogh, G.G. Tibbetts, F.E. Pinkerton, G.P. Meisner, C.H. Olk, J. Alloys Compd. 350 (2003) 135.
[12] Q.J. Fu, A.J. Ramirez-Cuesta, S.C. Tsang, J. Phys. Chem. B 110 (2006) 711.
[13] H. Clasen, Angew. Chem. 73 (1961) 322.
[14] M.J. Frisch, et al., Gaussian 03, Revision C. 02, Gaussian, Inc., Wallingford CT, 2004.
[15] B.C. Hauback, H.W. Brinks, C.M. Jensen, K. Murphy, A.J. Maeland, J. Alloys Compd. 358 (2003) 142.
[16] M.D. Segall, P.J.D. Lindan, M.J. Probert, C.J. Pickard, P.J. Hasnip, S.J. Clark, M.C. Payne, J. Phys. Condens. Matter 14 (2002) 2717.
[17] B.C. Hauback, H.W. Brinks, H. Fjellvåg, J. Alloys Compd. 346 (2002) 184.
[18] B.C. Hauback, H.W. Brinks, R.H. Heyn, R. Blom, H. Fjellvåg, J. Alloys Compd. 394 (2005) 35.
[19] H.W. Brinks, B.C. Hauback, J. Alloys Compd. 354 (2003) 143.
[20] E. Rönnebro, D. Noréus, K. Kadir, A. Reiser, B. Bogdanović, J. Alloys Compd. 299 (2000) 101.
[21] J.-C. Bureau, B. Bonnetot, P. Claudy, H. Eddaudi, Mater. Res. Bull. 20 (1985) 1147.
[22] M.W. Wong, Chem. Phys. Lett. 256 (1996) 391.
[23] G. Remaudin, S. Gomes, H. Hagemann, L. Keller, K. Yvon, J. Alloys Compd. 375 (2004) 98.
[24] A.E. Finholt, G.D. Barbaras, G.K. Barbaras, G. Urry, T. Wartik, H.I. Schlesinger, J. Inorg. Nucl. Chem. 1 (1955) 317.
[25] M. Mamula, T. Hanslík, Coll. Czechosolv. Chem. Commun. 32 (1967) 884.
[26] T.W. Turly, H.W. Rinn, Inorg. Chem. 8 (1996) 18.
[27] J.P. Maehlen, J.P. Maehlen, V.A. Yartys, R.V. Denys, M. Fichtner, Ch. Frommen, B.M. Bulychev, P. Pattison, H. Emerich, Y.E. Filinchuk, D. Chernyshov, J. Alloys Compd. 446–447 (2007) 280.
[28] V.A. Yartys, J.P. Maehlen, R.V. Denys, M. Fichtner, Ch. Frommen, B.M. Bulychev, H. Emerich, Y.E. Filinchuk, MH2006, O-73.